Deformation of Wrinkled Graphene

(Supporting Information)

Zheling Li[1], Ian A. Kinloch[1], Robert J. Young[1], Kostya S. Novoselov[2], George Anagnostopoulos[3], John Parthenios[3], Costas Galiotis[3,4], Konstantinos Papagelis[3,5], Ching-Yu Lu[6], Liam Britnell[6]*

[1]School of Materials and [2]School of Physics and Astronomy, University of Manchester, Oxford Road, Manchester, M13 9PL, UK

[3]Institute of Chemical Engineering Sciences, Foundation for Research and Technology – Hellas (FORTH/ ICE-HT), P.O. Box 1414, Patras 265 04, Greece,

[4]Department of Chemical Engineering and [5]Department of Materials Science, University of Patras, Patras 26504, Greece

[6]BGT Materials Ltd, Photon Science Institute, University of Manchester, Oxford Road, Manchester, M13 9PL, UK

1. Transfer of the CVD graphene to the PET substrate

The CVD graphene was transferred to PET using the well-known technique of chemical etching of copper in ferric chloride. The graphene/copper had a poly(methyl methacrylate) (PMMA) coating applied to the surface to act as a support during transfer. This was allowed to dry at room temperature. The backside graphene was removed by oxygen plasma. The PMMA/graphene/copper foil was then placed in ferric chloride until all copper was dissolved. The film was then subsequently transferred to three baths of DI water. The PMMA/graphene film was then fished from the last DI bath with a clean PET film and allowed to dry overnight. The PMMA/graphene/PET film was then soaked in acetone to remove the PMMA. The graphene/PET film was rinsed in IPA and blown dry with nitrogen as a final cleaning step.

2. Determination of the lateral dimensions of the graphene islands

The lateral dimension of each graphene island was estimated by averaging the length of two crossed lines across the island, as shown in Figure S1. Over 500 islands were measured in this way to give the statistical distribution in Figure 1(c). A typical example of this measurement is shown in Figure S1(b).

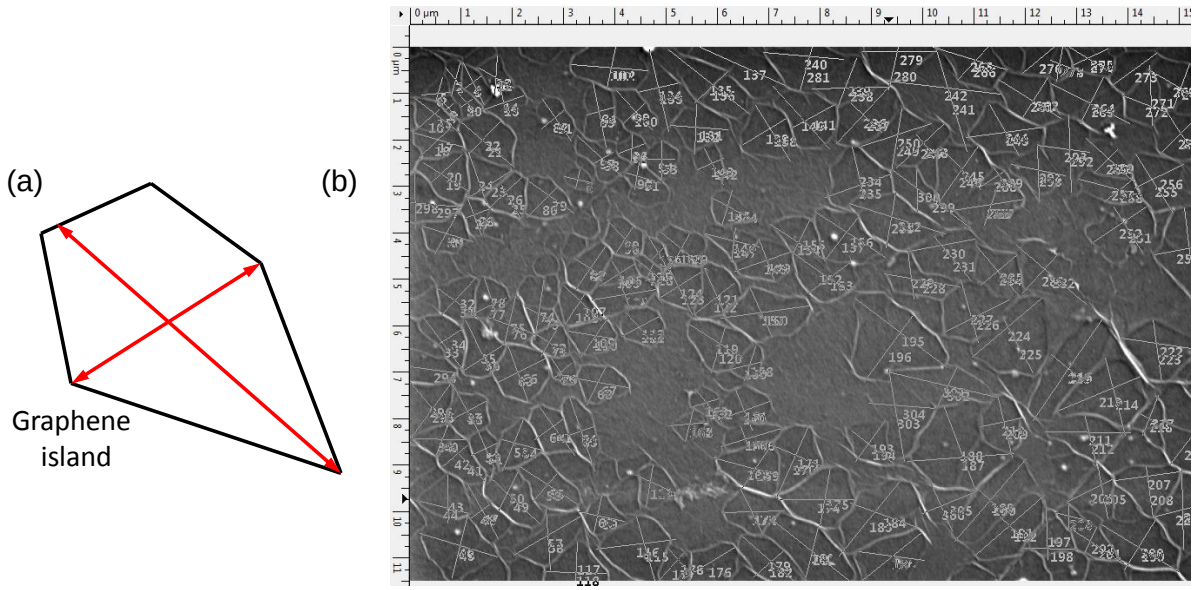

Figure S1. (a) Method employed to measure the lateral dimension of the graphene islands from SEM micrographs. The black line is the edge of graphene island, and its lateral dimension is measured by averaging the length of the two red lines across it. (b) A typical SEM micrograph showing the individual measurements.

3, The effect of wrinkles upon stress transfer

The AFM height scan in Figure 1(d) in the manuscript clearly shows that the wrinkles stick up above the PET substrate. As shown before for a different system, when the wrinkles form by a similar mechanism, the upper layer stick up and leave a hollowed region between the top and bottom layer.[1] Similarly in our situation, there will be a hollow region within the wrinkles in which there can be no stress transfer giving rise to the mechanically-isolated graphene islands and mechanically-free edges within the wrinkles because of the absence of the interface with the substrate, as shown schematically in Figure S2. Deformation will also lead to straightening of the wrinkles. It should be noted that the diagrams in Figure S2 are not to scale – the size of the islands (1.2 μm) is much larger than the height of the wrinkles (~20 nm).

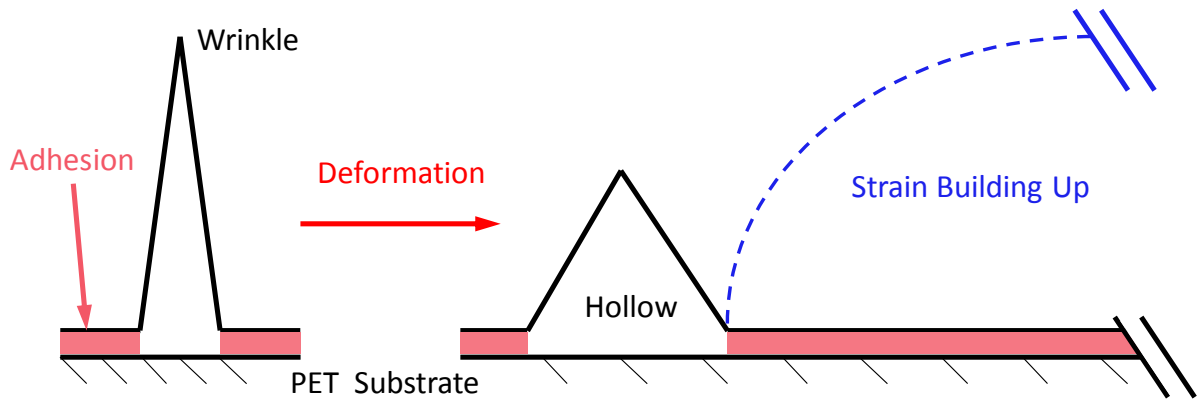

Figure S2. Schematic diagram of the deformation of the wrinkled structure (not to scale).

4. Determination of the mean rates of 2D Raman band shift and band broadening

The mean size of the graphene islands was fixed by the process used to produce the CVD graphene/PET material although Figure 1(c) shows that there was a wide distribution of sizes. Although we were not able to modulate the mean value, we were able to investigate the effect of variation in the lateral dimensions indirectly by undertaking measurements in random position on specimens as shown in Figure S3. It can be seen that there are wide variations in the rates of both band shift and band broadening for the 2D band. The 8 sets of data are more scattered than for similar measurement on flat mechanically-exfoliated graphene[2] and the difference in behavior is most likely due to the variations of lateral dimensions in the regions chosen at random.

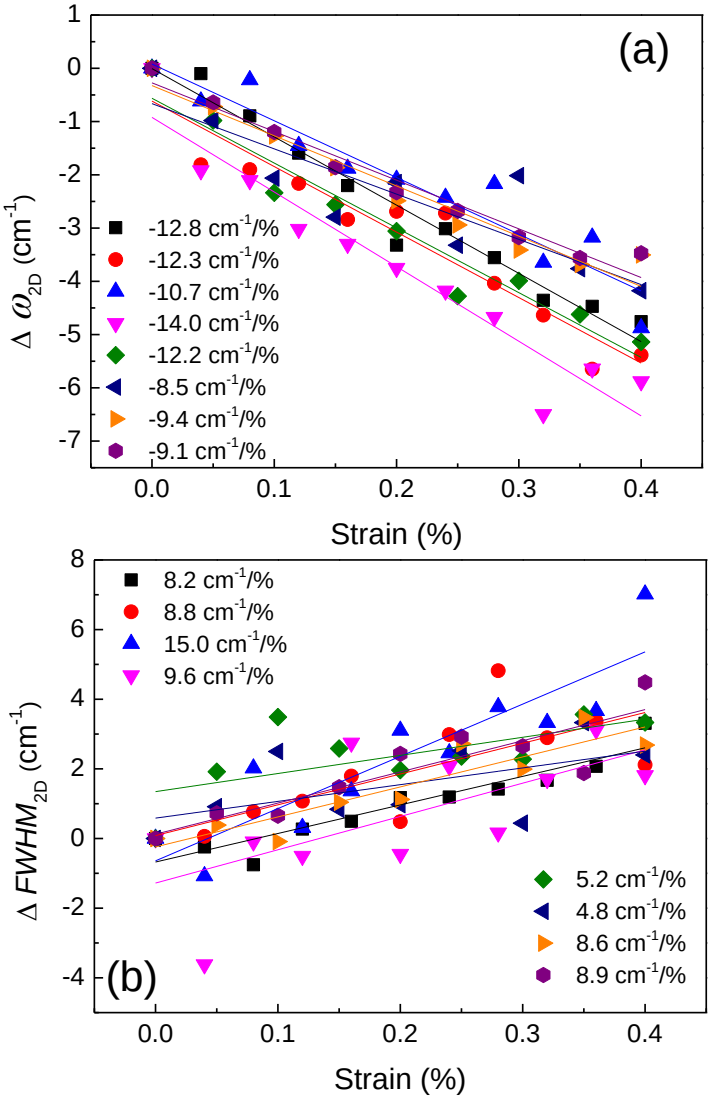

Figure S3. The variation of (a) ω_{2D} (b) $FWHM_{2D}$ as the function of strain in each test, with the $d\omega_{2D}/d\varepsilon$ and $dFWHM_{2D}/d\varepsilon$ also indicated.

The Raman spectra of a typical CVD graphene/PET specimen at different strain level are in shown in Figure S4.

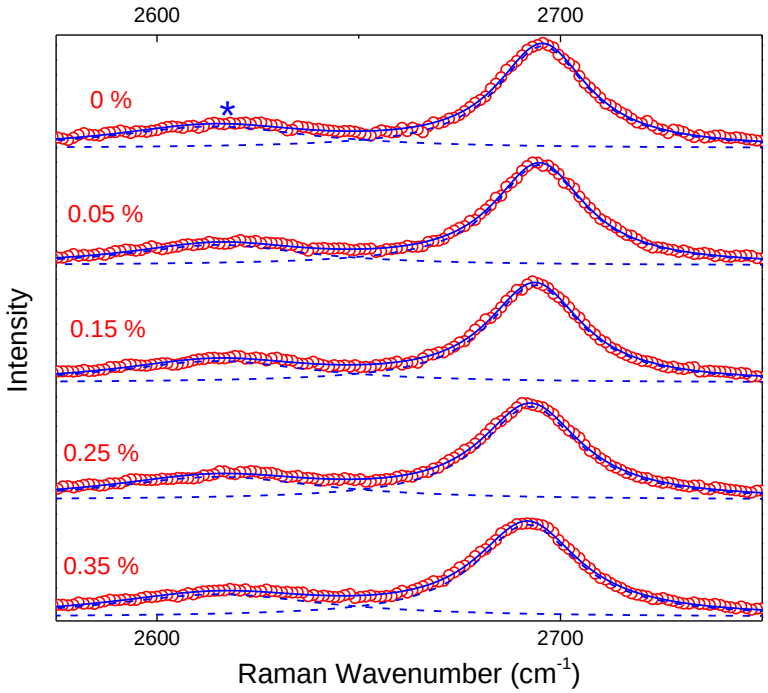

Figure S4. Raman spectra of the wrinkled CVD graphene on PET at different strain level. The red dots and blue curves denote the experimental spectra and curve fittings, respectively. The blue '*' indicates the Raman band from PET substrate.

5. The estimation of the laser spot size and the local laser intensity calculation

It can be assumed that the laser intensity $I(r)$ within the spot of a Gaussian laser beam follows the Gaussian distribution:[3]

$$I(r) = \exp\left(-2\frac{r^2}{r_0^2}\right) \qquad \text{(S1)}$$

where r is the distance to the laser spot center, and r_0 is the radius of the laser beam, defined as the radius of the plane where $I(r)$ decreases to $1/e^2$ of its maximum value.

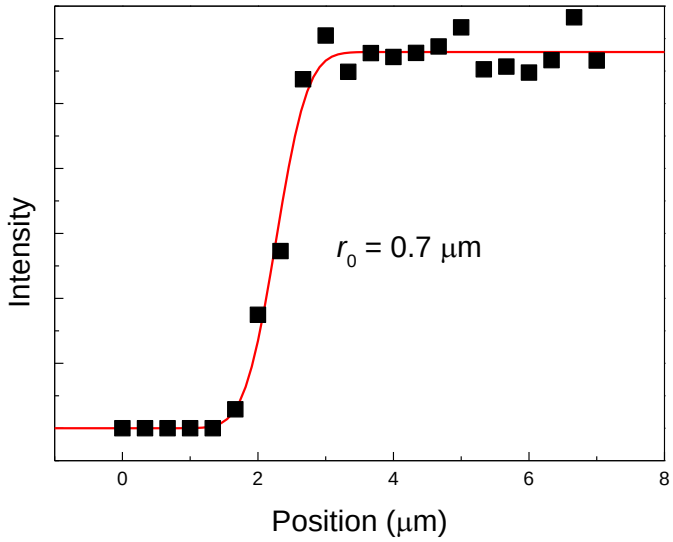

Figure S5. Variation of *I* when the laser beam is moving across a well-defined graphene edge.

The spot size of the Gaussian beam laser[3] was estimated by moving the laser spot inwards from outside a mechanical exfoliated monolayer graphene towards its center, and the 2D band intensity *I* can be fitted as the function of laser position x_l (Figure S5):[4]

$$I = \sqrt{\frac{\pi}{8}} A r_0 \left(1 + \mathrm{erf}\left(\frac{\sqrt{2}(x_l - x_0)}{r_0} \right) \right) \qquad \text{(S2)}$$

where x_0 is the graphene edge location and *A* is the amplitude. For regions where the 2D was not resolvable, *I* was set as zero. By fitting *I* with eq S2, the radius of the laser beam r_0 is obtained as ~0.7 μm. Thus diameter of the laser spot size is estimated to be 1.4 μm.[5]

If the distance between each unit (Figure 4(c)) is then calculated through the unit center, the local laser intensity at unit (*L*,*T*), $I_{\mathrm{laser}}(L,T)$ is given by modification of eq S1 as:

$$I_{\mathrm{laser}}(L,T) = \exp\left[-2 \cdot \frac{(0.1L - 0.05)^2 + (0.1T - 0.05)^2}{{r_0}^2} \right] \qquad \text{(S3)}$$

6. The effect of laser spot position and the *ns* values upon ω_{2D} and $FWHM_{2D}$

The effect of the exact laser spot position and the *ns* values to the variation of ω_{2D} and $FWHM_{2D}$ are also considered. The laser spot is approximated to a square and Figure S6 shows the situation where the laser spot is centred at the wrinkles. The overlapped region of graphene islands and laser spot contributes to the calculated Raman spectra, and only the region marked by dashed red lines was taken into calculation due to its symmetrical geometry.

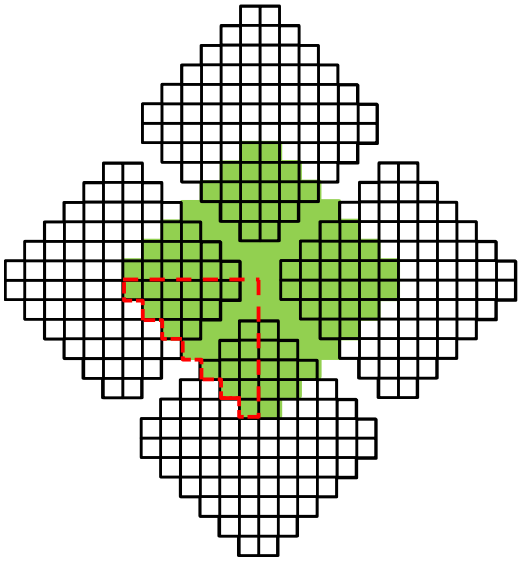

Figure S6. Schematic diagram of the laser spot (approximated to a square) centered at the wrinkles (the gaps) between the graphene islands (black squares). The overlapped region of graphene islands and laser spot (green square) contributes to the calculated Raman spectra.

The effect of the exact laser spot position and the *ns* values to the variation of ω_{2D} and $FWHM_{2D}$ are shown in Figure S7.

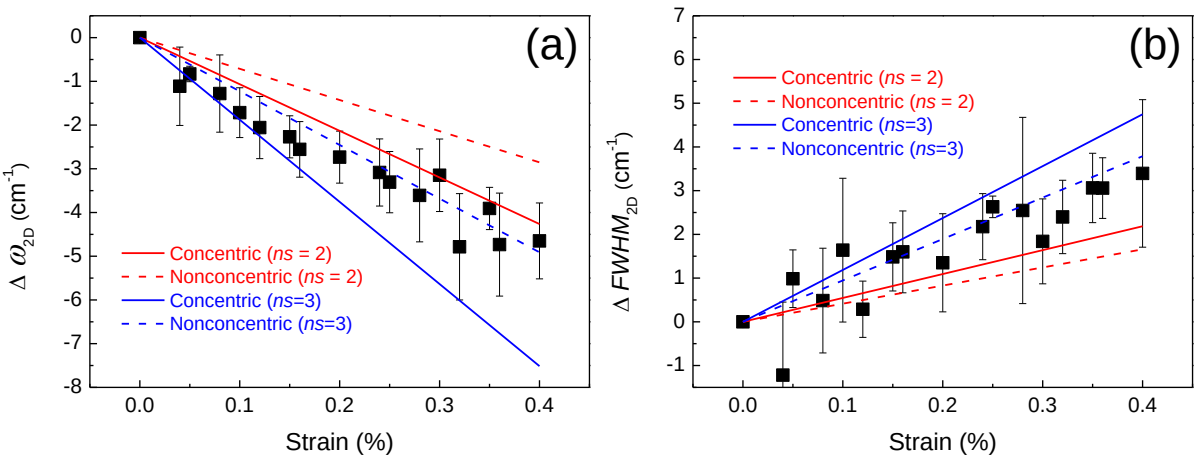

Figure S7. Predicted variation of (a) ω_{2D} (b) $FWHM_{2D}$ as the function of strain when graphene island and laser spot are concentric (solid lines) and nonconcentric (dashed lines), with an *ns* value of 2 (red lines) and 3 (blue lines). Black squares are the experimental results.

It can be seen that the experimental data can be fitted by choosing the appropriate combination of spot position (concentric or nonconcentric) and *ns* values.

REFERENCES

1. Adelung, R.; Ernst, F.; Scott, A.; Tabib-Azar, M.; Kipp, L.; Skibowski, M.; Hollensteiner, S.; Spiecker, E.; Jäger, W.; Gunst, S.; *et al.* Self-Assembled Nanowire Networks by Deposition of Copper onto Layered-Crystal Surfaces. *Adv. Mater.* **2002,** *14*, 1056-1061.

2. Young, R. J.; Gong, L.; Kinloch, I. A.; Riaz, I.; Jalil, R.; Novoselov, K. S. Strain Mapping in a Graphene Monolayer Nanocomposite. *ACS Nano* **2011,** *5*, 3079-3084.

3. Siegman, A. E. *Lasers*; University Science Books: Sausalito: California, 1986.

4. Gupta, A. K.; Russin, T. J.; Gutiérrez, H. R.; Eklund, P. C. Probing Graphene Edges via Raman Scattering. *ACS Nano* **2008,** *3*, 45-52.

5. Cai, W.; Moore, A. L.; Zhu, Y.; Li, X.; Chen, S.; Shi, L.; Ruoff, R. S. Thermal Transport in Suspended and Supported Monolayer Graphene Grown by Chemical Vapor Deposition. *Nano Lett.* **2010,** *10*, 1645-1651.